Mesoscopic Transport in Chemically Doped Carbon Nanotubes

Sylvain Latil,[1,*] Stephan Roche,[2] Didier Mayou,[3] and Jean-Christophe Charlier[1]

[1]*PCPM and CERMIN, Université Catholique de Louvain, Place Croix du Sud 1, B-1348 Louvain-la-Neuve, Belgium*
[2]*Commissariat à l'Energie Atomique, DSM/DRFMC/SPSMS, 17 avenue des Martyrs, F-38054 Grenoble Cedex 9, France*
[3]*LEPES, 25 avenue des Martyrs, BP 166, F-38042 Grenoble Cedex, France*

(Received 8 January 2004; published 25 June 2004)

Electronic quantum transport is investigated in boron- and nitrogen-doped carbon nanotubes using tight-binding methods correlated to *ab initio* calculations. The present technique accurately accounts for both effects of dopants, namely, charge transfer and elastic scattering. Generic transport properties such as conduction mechanisms, mean-free paths, and conductance scalings are derived for various concentration of randomly distributed boron and nitrogen dopants. Our calculations allow direct comparison with experiments and demonstrate that a small amount of dopants ($<0.5\%$) can drastically modify the electronic transport properties of the tube, which is certainly a key effect feature for envisioning nanoelectronics.

DOI: 10.1103/PhysRevLett.92.256805 PACS numbers: 73.63.Fg, 71.55.–i

Since their discovery in 1991 [1], carbon nanotubes (CNTs) have sparked off a tremendous amount of activities from basic science to applied technologies. In particular, depending on their geometrical helicity, CNTs can be either metallic or semiconducting with an anticipated diameter-dependent energy gap scaling [2]. In addition to their unusual electronic spectrum, these systems also exhibit remarkable quantum transport properties [3,4], which present them as serious candidates for emerging nanoelectronics [5]. In view of incorporating CNTs into real operational nanodevices (diodes, transistors), CNT-based intramolecular junctions were proposed early on [6]. Both theoretical [7] and experimental [5,8] studies of such nanojunctions are full of promise.

In order to tailor the electronic properties of CNTs, the Fermi level can be tuned by chemical doping [9]. Carbon nanotubes doped either with nitrogen or boron [10–12] substitutions have been synthesized. When substituting a carbon atom, the boron atom (nitrogen) acts as an acceptor (donor) impurity in the nanotube, as revealed by thermopower measurements [13]. First-principle studies of the electronic structure [14] and quantum transport in boron-doped (nitrogen) carbon nanotubes using the Landauer [15] and Keldysh [16] formalisms have revealed the presence of localized states around the substituting impurity. These quasibounded states are responsible for an enhancement of the backscattering for energies below (above) the charge neutrality point. However, due to computational limitations of the *ab initio* techniques, these approaches have been so far restricted to short devices containing a single doping atom. As a result, little is known about intrinsic transport length scales at the Fermi level in such hetero-atomic nanostructures. First experimental transport measurements [17,18] have been recently reported in boron-doped nanotubes with typically a few percent of dopants for metallic nanotubes with mesoscopic length scales. In particular, K. Liu *et al.* [17] describe electrical transport in boron-doped nanotubes by means of weak localization theory and estimate mean-free paths in the order of 220–250 nm, for nanotubes with diameters in the range 17–27 nm and for a few percent of boron dopants. In this Letter, generic transport properties of boron- and nitrogen-doped nanotubes, such as conduction mechanisms, mean-free paths and conductance scalings, are computed as a function of the density of dopants.

Electronic calculations have been carried on large structures (between 10 nm and 1 μm long), where only the semiempirical Hamiltonians and order N techniques are appropriate. Consequently, the zone folding (ZF) technique has been used. This method is an orthogonal tight-binding (TB) approach, which takes into account only one orbital ($p_\perp$) per carbon atom and describes correctly the usual electronic properties of pristine carbon nanotubes (gaps, positions of Van Hove singularities, Fermi velocity, etc. [2]). The presence of the gap, due to the local curvature, in the band structure of "metallic" nanotubes [19] is not predicted by ZF calculations, but since this work addresses doped systems, a truly metallic behavior should be recovered.

Within this framework, the Hamiltonian operator writes as follows:

$$\hat{\mathbf{H}} = \sum_{n=1}^{N}\left[H_{nn}|n\rangle\langle n| + H_{np}\sum_{p}|n\rangle\langle p| \right], \qquad (1)$$

where the first sum runs on all the $p_\perp$ orbitals in the system, while the second sum runs on the first neighbors of the n site. In expression (1), the matrix elements H_{nn} are the on-site energies and H_{np} are the hopping integrals.

In order to apply this ZF technique to B- and N-doped carbon nanotubes, the electronic properties in the vicinity of an atomic substitution need to be accurately described. Tight-binding methods are usually not suitable to predict

the charge transfer, especially in the case of heteroatomic substitutions. However, by adding a corrective electrostatic potential to the on-site energies, this technique can handle electric fields, charge transfer, or electric dipole moments. The correction (added to the on-site energies) is usually calculated by a self-consistent loop on the electric charge [20]. Unfortunately, as the present $O(N)$ technique does not allow one to use such a self-consistent scheme, an alternative approach is explained below for the case of a B-doped CNT (N doping follows an analogous procedure)

In our modified ZF model, the value of the matrix elements in Eq. (1) are supposed to vary, depending on the involved species. These elements are labeled ε_C, ε_B, etc., (for the on-site energies H_{nn}) and γ_{CC}, γ_{BC}, etc., (for the hopping integrals H_{np}). Practically, these parameters were defined by fitting the ZF band structure on DFT-LDA (density-functional theory, local-density approximation) calculations [21]. In this *ab-initio* approach, standard norm-conserving pseudopotentials were used, and the cutoff energy for the plane waves expansion was set to $E_{\text{cut}} = 30$ hartree. Since the curvature of the graphene sheet is neglected within ZF calculations, the LDA calculations were performed on flat "graphenelike" systems. At first, the electronic structure of a supercell containing 31 carbon atoms and a single B atom was studied within a spin-averaged LDA approach in order to simulate the electronic states of a doped carbon system in the vicinity of the B impurity. As shown in Fig. 1(a), the electronic density $\rho(r)$ for the last (half) occupied band is distributed only on the $p_\perp$ orbitals for atoms located close to the impurity, up to the third neighbor of the B atom. This localization of the HOMO-LUMO (highest occupied molecular orbital, lowest unoccupied molecular orbital) band allows one to consider that the correction on the on-site energies effects carbon atoms only up to the third neighbors of the impurity. Moreover, this result suggests that the hopping integral between sites will not be effected by the charge transfer in assumption that the p atomic orbitals are not polarized by the local electric field. In addition, the boron atom is supposed to be "carbonlike" [22], i.e., $\gamma_{CC} = \gamma_{BC} = \gamma$. The geometry of the model is presented in Fig. 1(b), where the boron and the renormalized carbon atoms are labeled. In this situation, only six parameters require adjustment: the unique hopping integral γ, the carbon and boron on-site energies ε_C and ε_B, and the renormalized carbon on-site energies ε_3, ε_2, and ε_1 [third, second, and first neighbors of the boron atom, respectively, as shown in Fig. 1(b)].

These adjustments were performed using a least square energy minimization scheme between LDA and ZF band structures. At first, the LDA electronic structure of an isolated graphene sheet was used to fit the hopping. Its value (see Table I) was kept further as a constant. As only a low density of boron atoms in a graphene sheet is considered, and given that this supercell is supposed to be in electronic equilibrium with the surrounding nanotube, the chemical potentials (Fermi energies) of the two subsystems have to be equal. Since the Fermi energy of a graphene sheet (or a nanotube described with ZF technique) is ε_C, this leads to $\varepsilon_C = E_{F,\text{supercell}} = E_{F,\text{CNT}}$. The band structure obtained with the optimal parameters is compared to the LDA band structure in Fig. 1(c). These optimal parameters for B-doped (and N-doped) are given in Table I.

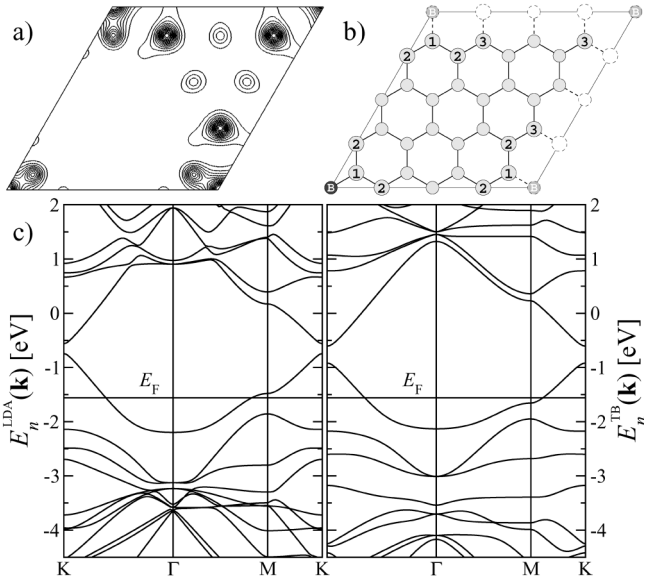

FIG. 1. Electronic properties of a boron substitution in a graphene sheet. (a) Isodensity plot of the last (half) occupied band, at Γ point calculated with DFT-LDA. The plane is shifted from the graphitic sheet (0.625 Å). Electronic density is mainly distributed on the B atom, until the third neighbor. (b) The renormalized atoms used our model are labeled: 1st, 2nd, and 3rd neighbors of the boron (B) atom. (c) Comparison between the electronic band structures of the doped graphene sheet calculated with DFT-LDA (left) and our modified ZF model (right) with the renormalized on-site energies (see text).

In order to fit with experimental data [23], a global scaling is applied to the parameters, recovering $\gamma = \gamma_0 = 2.9$ eV and the whole spectrum is shifted to have $E_F = 0$ eV. As shown in Fig. 2(a), the density of states (DOS) of a (0.1%) B-doped (10,10) CNT exhibits the typical acceptor peak (E_1), in agreement with previous *ab initio* studies [15].

Conduction properties of a single B CNT (or N CNT) are estimated using the Kubo formalism. This approach is

TABLE I. Renormalized on-sites energies used in this work (in eV). Hopping integral $\gamma = 2.72$ eV and Fermi level $E_F = \varepsilon_C$ for both cases.

	$\varepsilon_B/\varepsilon_N$	ε_1	ε_2	ε_3	ε_C
B doping	+2.77	−0.16	+0.21	+0.39	−1.56
N doping	−2.02	−3.06	−1.98	−2.12	−0.08

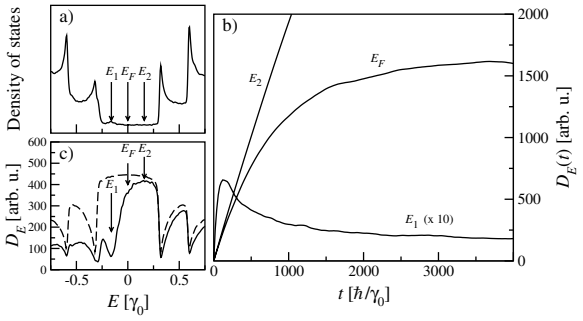

FIG. 2. Electronic diffusion in a (0.1%) B-doped (10,10) CNT. (a) Density of states illustrating the characteristic acceptor peak located below the Fermi level (here $E_F = 0$). (b) Diffusivity $D_E(t)$ given by Eq. (4), as a function of time for the three energies, indicated by arrows in (a). The difference of diffusion, according to the conduction regime is clear: ballistic (E_2), diffusive (E_F), and localized (E_1, for which the coefficient is 10 times magnified). (c) The diffusivity D_E plotted as a function of energy (at the time $t = 200\hbar/\gamma_0$) for the same B-doped CNT (solid line) and a pristine CNT (dashed line).

based on the fluctuation-dissipation theorem, which establishes that the nonequilibrium linear response (conductivity) is related to the equilibrium correlation function of the carrier velocities. In the real-space approach the transport properties are associated with the measure of the quadratic time spreading $\Delta X_E(t) = \sqrt{\langle X^2(t)\rangle_E}$ of the electrons [24]. Following previous works [25], the spreading reads

$$\langle X^2(t)\rangle_E = \frac{\langle \mathrm{wp}|A^\dagger(t)\delta(E-\hat{\mathbf{H}})A(t)|\mathrm{wp}\rangle}{\langle \mathrm{wp}|\delta(E-\hat{\mathbf{H}})|\mathrm{wp}\rangle}, \qquad (2)$$

where $A(t) = [\hat{\mathbf{X}}, \exp(-i\hat{\mathbf{H}}t)]$, $\hat{\mathbf{H}}$ is the Hamiltonian operator, and $\hat{\mathbf{X}}$ is the position operator in the Schrödinger representation. The expectation values are calculated on wave packets $|\mathrm{wp}\rangle$ that are treated as random-phase states [26]:

$$|\mathrm{wp}\rangle = \frac{1}{\sqrt{N}}\sum_{n=1}^{N} e^{2i\pi\alpha(n)}|n\rangle, \qquad (3)$$

where $\alpha(n)$ is a random number in the $[0, 1]$ range. The choice of an orthogonal basis set (in the ZF approach) simplifies the expectation value of the position operator, assuming that $\langle n|\hat{\mathbf{X}}|p\rangle = \delta_{np}x_n$. Finally, to obtain the evolution of $A(t)|\mathrm{wp}\rangle$, the time-dependent Schrödinger equation is numerically solved by expanding the evolution operator on a Chebychev polynomials basis set [24,27], whereas the spectral measures are computed by recursion [28].

The spreading (2) is the key quantity as it is directly related to the diffusion coefficient (or diffusivity) whose time dependence fully determines the transport mechanism and the conductance scaling:

$$D_E(t) = \langle X^2(t)\rangle_E \frac{1}{t}. \qquad (4)$$

In Fig. 2, three different transport regimes are illustrated for a (0.1%) B-doped nanotube. At Fermi energy (E_F), while the density of states [in Fig. 2(a)] remains unaffected, the diffusion coefficient [in Fig. 2(b)] saturates at long times where $D(E_F, t) \to D_0 \sim \ell_e v_F$, indicating a diffusive regime. In contrast, at the resonance energy (E_1) of the quasibounded states, the diffusivity exhibits an $\sim 1/t$ behavior, typical of a strong localization regime. Finally, at energy E_2 above the Fermi level, the electronic conduction remains nearly insensitive to dopants, as shown by the quasiballistic diffusion law. In Fig. 2(c), the energy-dependent diffusivity clearly manifests such asymmetry in conduction.

From a physical point of view, the relevant information is that a low density of dopants yields diffusive regimes, with a mean-free path decreasing linearly with dopant concentration following Fermi golden rule (Fig. 3, left) and increasing linearly with nanotube diameter (Fig. 3, right) following theoretical predictions based on Anderson-like disorder modeling [3]. Moreover, in very good agreement with experimental data [17], from our calculations we estimate mean-free paths in the order of 175–275 nm for boron-doped nanotubes with diameters in the range 17–27 nm and 1.0% of doping.

The conductance scaling in the quantum coherent regime [29] is now analyzed in both boron and nitrogen doping cases. From the Kubo formula, the generic conductance of a device of length L_{dev} writes [30]

$$G(E, L_{\mathrm{dev}}) = 2e^2 n(E)\frac{D_E(\tau_{\mathrm{dev}})}{L_{\mathrm{dev}}}, \qquad (5)$$

where $n(E)$ is the electronic DOS per unit length and $\tau_{\mathrm{dev}}(E)$ is the time spent by the wave packet (at the considered energy E) to spread over a distance equal to L_{dev}. Following the fluctuation-dissipation framework, it is also equivalent to the time needed by an electron to travel through the device [31].

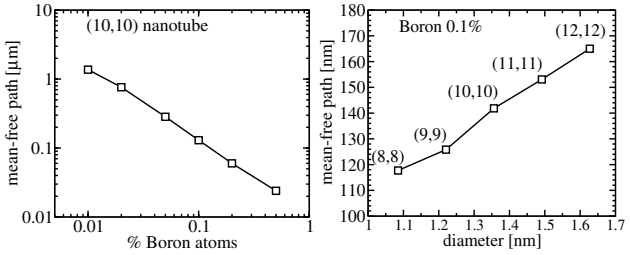

FIG. 3. Scaling of the mean-free path ℓ_e at the Fermi level, for a B-doped (n, n) nanotube. Left: in the case of a (10,10) nanotube with various boron concentrations, ℓ_e behaves like the inverse of the doping rate. Right: for a fixed concentration of B atoms, ℓ_e is roughly a linear function of the diameter.

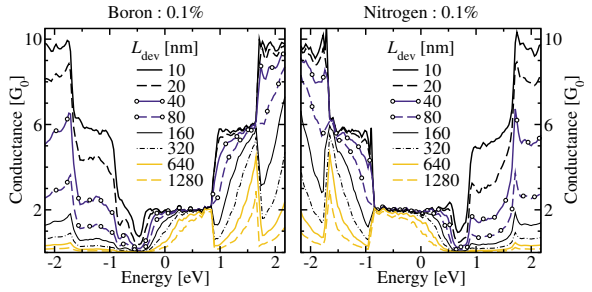

FIG. 4 (color online). Quantum conductance of a device made from a single (10,10) nanotube containing 0.1% of boron (left) or nitrogen (right) impurities. The conductance is plotted as a function of the energy, for different lengths of the device. A decrease of the conductance is observed near the energies of donor/acceptor states and near the Van Hove singularities.

The main remarkable conductance features for B- and N-doped (10,10) nanotubes are illustrated in Fig. 4. In both case, as the typical length L_{dev} increases from the nanometric scale ($\sim$10 nm) to the mesoscopic scale ($\sim 1\ \mu$m), the quantum interference effects beyond the diffusive regime are correspondingly enhanced. A strong asymmetric damping of the electronic conductance follows.

Moreover, our results show that the generic conductance $G(E, L_{dev})$ of B (N) CNT at Fermi level exhibit a positive (negative) derivative with respect to energy. Such a difference between N- and B-doped CNTs suggests that the thermopower measurements originate from a diffusion mechanism only [13]. Gate-dependent studies on individual undoped carbon nanotubes have recently revealed a quantum connection between conductance modulations and thermopower [32]. Similar studies on chemically doped CNTs would be desirable to confirm our theoretical predictions.

In conclusion, the energy-dependent quantum transport properties of chemically doped carbon nanotubes have been investigated. By combining first principle methods to tight-binding approaches, the mean-free path and the length-dependent conductance scalings were derived by simultaneously taking into account the chemical nature of impurities together with their random distribution over micrometer length scales. This gives a theoretical framework for understanding experiments.

The authors are grateful to F. Triozon and X. Gonze for valuable discussions. J. C. C. acknowledges the Belgian FNRS for financial support. The present work was carried out within the framework of the COMELCAN Project (European RTN, HPRC N-CT-2000-00128), the Program on Inter-University Attraction Poles (PAI 5/1/1), and the ARC of the Communauté Française de Belgique.

*Present address: Department of Chemistry, University of Sussex, Falmer, Brighton BN1 9QJ, United Kingdom.

[1] S. Iijima, Nature (London) **354**, 56 (1991).
[2] R. Saito, G. Dresselhaus, and M. S. Dresselhaus, *Physical Properties of Carbon Nanotubes* (Imperial College Press, London, 1998).
[3] C. T. White and T. N. Todorov, Nature (London) **393**, 240 (1998).
[4] S. Frank *et al.*, Science **280**, 1744 (1998).
[5] C. Zhou *et al.*, Science **290**, 1552 (2000); V. Derycke *et al.*, Nano Lett. **1**, 453 (2001).
[6] B. I. Dunlap, Phys. Rev. B **49**, 5643 (1994).
[7] V. Meunier, L. Henrard, and P. Lambin, Phys. Rev. B **57**, 2586 (1998).
[8] Z. Yao *et al.*, Nature (London) **402**, 273 (1999).
[9] J. E. Fischer, Acc. Chem. Res. **35**, 1079 (2002).
[10] M. Terrones *et al.*, Chem. Phys. Lett. **257**, 576 (1996).
[11] R. Czerw *et al.*, Nano Lett. **1**, 457 (2001).
[12] D. L. Carroll *et al.*, Phys. Rev. Lett. **81**, 2332 (1998).
[13] Y.-M. Choi *et al.*, Nano Lett. **3**, 839 (2003).
[14] A. H. Nevidomskyy, G. Csányi, and M. C. Payne, Phys. Rev. Lett. **91**, 105502 (2003).
[15] H. J. Choi *et al.*, Phys. Rev. Lett. **84**, 2917 (2000).
[16] C.-C. Kaun *et al.*, Phys. Rev. B **65**, 205416 (2002).
[17] K. Liu *et al.*, Phys. Rev. B **63**, 161404 (2001).
[18] V. Krstic *et al.*, Phys. Rev. B **67**, 041401 (2003).
[19] M. Ouyang *et al.*, Science **292**, 702 (2001).
[20] C. Krzeminski *et al.*, Phys. Rev. B **64**, 085405 (2001).
[21] DFT-LDA calculations were performed with ABINIT software. X. Gonze *et al.*, Comput. Mater. Sci. **25**, 478 (2002).
[22] Since the electronic density for a carbon and a boron (or nitrogen) atom at a distance $d = 1.42$ Å is roughly the same, this approximation is valid.
[23] G. Dresselhaus *et al.*, in *Science and Application of Nanotubes*, edited by D. Tománek and R. J. Enbody (Kluwer Academics, New York, 2000).
[24] S. Roche, Phys. Rev. B **59**, 2284 (1999).
[25] F. Triozon *et al.*, Phys. Rev. B **65**, 220202 (2002).
[26] An average over 20 random phases states was performed.
[27] The chosen time step is $\delta t = 20\hbar/\gamma_0 \simeq 4.5$ fs. In this case, the evolution operator is well approximated by a polynomial of degree $N_{poly} = 120$.
[28] R. Haydock, V. Heine, and M. J. Kelly, J. Phys. C **5**, 2845 (1972).
[29] Beyond this independent-electrons model, phonons and electronic interactions lead to a finite phase coherent length. We assume that this length is always longer than the length of the device.
[30] S. Roche and R. Saito, Phys. Rev. Lett. **87**, 246803 (2001).
[31] This approach is equivalent to the Landauer formula, assuming reflectionless contacts. D. Fisher and P. A. Lee, Phys. Rev. B **23**, 6851 (1981).
[32] J. P. Small, K. M. Perez, and P. Kim, Phys. Rev. Lett. **91**, 256801 (2003).